Effect of Fault Depth on Near-Fault Peak Ground Velocity

Yanyan Yu, Haiping Ding, Pengjun Chen, Yiou Sun

Abstract—Fault depth is an important parameter to be determined in ground motion simulation, and peak ground velocity (PGV) demonstrates good application prospect. Using numerical simulation method, the variations of distribution and peak value of near-fault PGV with different fault depth were studied in detail, and the reason of some phenomena were discussed. The simulation results show that the distribution characteristics of PGV of fault-parallel (FP) component and fault-normal (FN) component are distinctly different; the value of PGV FN component is much larger than that of FP component. With the increase of fault depth, the distribution region of the FN component strong PGV moves forward along the rupture direction, while the strong PGV zone of FP component becomes gradually far away from the fault trace along the direction perpendicular to the strike. However, no matter FN component or FP component, the strong PGV distribution area and its value are both quickly reduced with increased fault depth. The results above suggest that the fault depth have significant effect on both FN component and FP component of near-fault PGV.

Keywords—Fault depth, near-fault, PGV, numerical simulation.

I. Introduction

STUDIES showed that the PGV has good application prospect in earthquake engineering [1]-[5], such as in estimating the probability of seismic-induced land-slide, in the predicting of seismic intensity, in the determining of site liquidation, in the evaluating of damage degree of buried pipelines in earthquake, etc. Subsequently, for the near fault region that frequently suffered the most severe damage, the investigation of the near fault PGV distribution feature has a good guidance value in the rapid assessment of earthquake disasters. The methods are roughly divided into two categories. One is statistical analysis by using the real strong ground motion records. Although quite a number of near fault seismic records have been obtained in recent large earthquakes such as the Chichi earthquake, the Wenchuan earthquake, etc., the record is obviously insufficient for the studying of regional PGV distribution, especially for considering different source parameters. The other one is the numerical simulation method [6]-[8], which can take the source rupture process, the propagation path, and the site condition into consideration. Besides, the source values can be changed according to the research need. So, the numerical method has become a powerful tool in the studying of near field strong ground motion, and is also the research focus currently. In this study,

Yanyan Yu, Haiping Ding and Yiou Sun are with the Key Laboratory of Structure Engineering of Jiangsu Province, Suzhou University of Science and Technology, Suzhou 215011, China.

Pengjun Chen is with the East China Mineral Exploration Development Bureau, Nanjing, 210007, China.

the variation pattern of the magnitude and the distribution feature of near fault PGV are investigated by using the numerical simulation method, the kinetic source model, and simple velocity model. Then, the inherent reason of the variation pattern is thoroughly discussed. The results of this paper can provide a reference for near field strong ground motion prediction.

II. Calculation Method and Model

A. Calculation Method

The software package of COMPSYN for earthquake ground motion simulation is used in our study. The programs are publicly released by the International Association of Seismology and Physics of the Earth's Interior (IASPEI). It uses the discrete wavenumber/finite element method (DWFE) [9] to calculate the Green's functions, and the synthetic seismograms are obtained by the convolution of the Green's functions with the slip space-time function on the fault plane. This integral can be solved by adaptive numerical integration techniques [10]. These programs have two primary strengths. First, the Green's functions include the complete response of the Earth structure, so that all P and S waves, surface waves, leaky modes, and near-field terms are included in the calculated seismograms. Second, the codes assume a 1D layered velocity structure, so they are computationally fairly fast compared to 3D codes, so that the user can simulate ground motions from many hypothetical rupture models in minimal time. The main omission is that anelastic attenuation cannot be modeled using these codes. We use this software to simulate the near field ground motion under different focal depth, and the effects of this parameter on near fault PGV distribution.

B. Calculation Model

To highlight the effect of fault depth on near fault PGV distribution, the source and velocity models are all quite simple. The fault is a vertical strike-slip fault with a rectangle shape and length of 12 km and width of 8 km. The initial rupture point locates at the middle of fault left boundary, and the rupture direction is from left to right. The buried depth of the fault upper boundary is 2 km. The source model is shown in Fig. 1 (a). For comparison convenience in the following with changing fault depth, this source model is referred to as the basic source model hereafter.

Fig. 1 (b) describes the distribution of observation points at the surface. Considering the rapid change of seismic motion at the near fault region [11], the observation points are denser for this region compared with the outside zone. There are totally

659 observation points in simulations.

To reduce the effect of propagation medium as small as possible, a homogeneous isotropic elastic halfspace is used in study, with a P-wave velocity of 5.196 km/s, an S-wave velocity of 3.0 km/s, and a density of 2000 kg/m³.
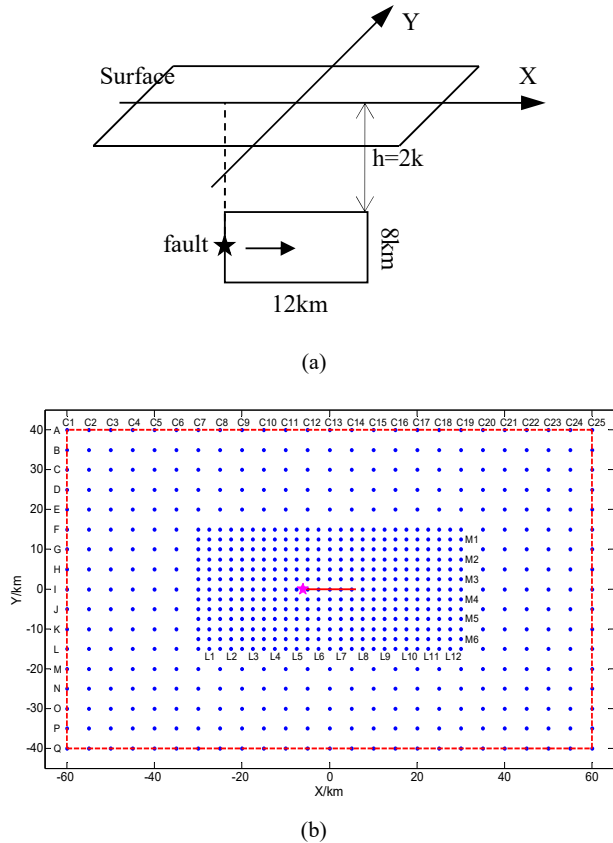

(a)

(b)

Fig. 1 (a) Sketch of source model. The fault length and width are 12 km and 8 km, respectively. The buried depth is 2 km.The star indicates the location of rupture starting point. The rupture speed equals 0.9 times of shear wave velocity, and the displacement is 0.35 m for every point on the fault, the rise time 0.45 s and the rake 0°. (b) Sketch of observation points distribution. The region surrounded by red dashed line represents the calculation region. The red solid line and star indicate the projection of fault and initial rupture point, respectively. The blue points denote observation points, which are numbered by rows and columns

III. Results of the Basic Model

Based on the calculation model of section 1.2, the velocity seismograms of FP, FN, and vertical component are calculated by using the software packages of COMPSYN. Then, the PGV distributions of the FP and FN component are obtained by using interpolation method, which are shown in Fig. 2.

The following can be observed from Fig. 2: (1) The velocity peak value of the FN component is much larger than the FP component, which is due to the rupture directivity effect, and is validated by the observations. (2) It is quite different for the distribution features of PGV of the FP and FN component. For the FP component, the strong PGVs depart from the fault trace

with some distance, and they are located both at the epicentral region and in front of the rupture direction. The largest PGV occurs near the epicenter, with an angle of 45° to the fault trace. However, for the FN component, the PGV distribution is dominated by the rupture directivity effect, strong PGVs mainly locate in front of the rupture direction, and the largest PGV occurs just at the fault trace in front of the rupture direction. The difference of the distribution characteristics between the FP and FN component mainly results from the source radiation pattern in the two directions [12].
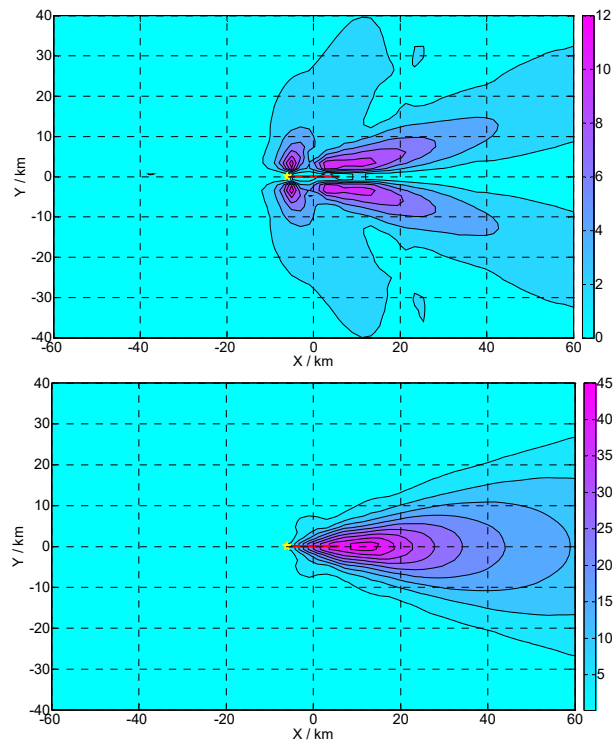

Fig. 2 The distribution map of PGV FP component (top) and FN component (bottom) for basic fault model, the units in the map are cm/s

IV. Effect of Fault Depth on Near-Fault PGV

Based on the basic model, the fault depth h changes gradually from 2 km to 9 km, with the other parameters keep unchanged. Then, the near-fault PGV distributions of the FN and FP component under different source depth are numerically obtained, as shown in Fig. 3 and Fig. 4, respectively. The yellow solid line and the red star denote the fault trace and the projection of the initial rupture point on the surface. To emphasize the change of PGV distributions for increasing source depth, the isolines in Figs. 3 and 4 are starting from 2 cm/s, and the white regions represent the PGV values less than 2 cm/s.

It is shown in Figs. 3 and 4 that, with the increase of fault depth, the strong PGV areas decrease rapidly both for the FN and FP component. Besides, it is also shown that, with the increase of fault depth, the strong PGV regions of the FN component move forward along the rupture direction, which

can be explained by the isochrone theory [8]. Isochrones are the locus of points on the fault that radiate elastic waves all of which arrive at a given station at the same time. According to this theory, a strong phase is radiated from the isochrone that is tangent to a barrier because the isochrone gets discontinuous at this point (the point at which the isochrone is first tangent to the top of the fault is called the critical point), which is always associated with a peak velocity or acceleration value at the free surface station very close to the critical point. Fig. 5 shows the relationship between the X coordinates of observation points (Xs) of line I and the corresponding X coordinates of the critical points (Xc). It can be observed from

Fig. 5 that, when the stations move forward along the fault strike, the critical points move forward accordingly. However, after Xs reaches a value, the value of Xc is almost fixed, and the critical point roughly stays at a same position, which is called the limiting position of the critical point. It is shown in Fig. 5 that, for the case of large fault depth, the Xs values of the limiting position of the critical point are obviously larger compared with the small fault depth case. Additionally, considering the strong geometrical attenuation (1/R) for the near-fault strong ground motion, the strong PGV regions of the FN component will move forward along the rupture direction with the increase of fault depth.
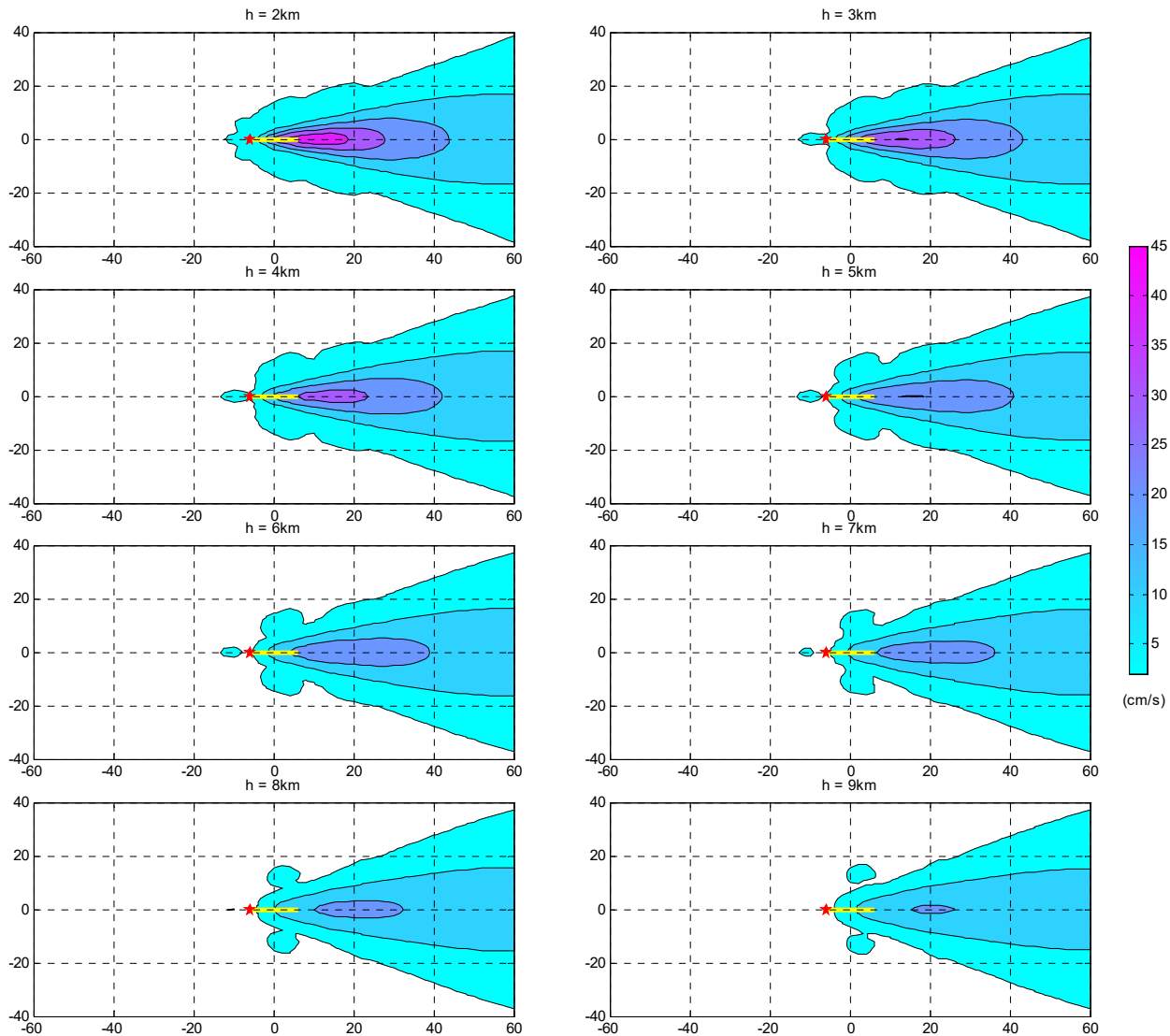

Fig. 3 The distribution map of PGV FN component for different fault depth
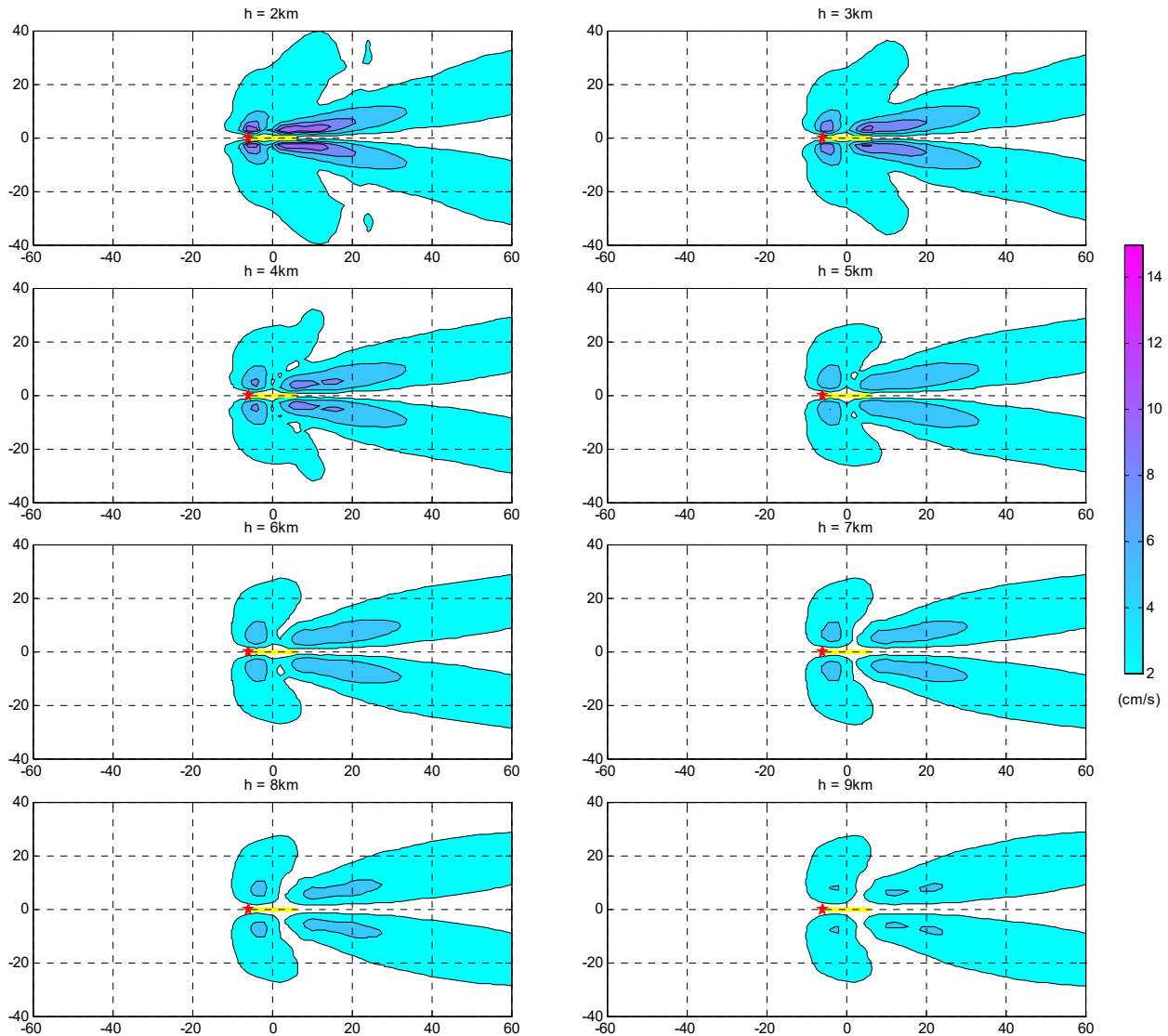
Fig. 4 The distribution map of PGV FP component for different fault depth

It can be observed from Fig. 4 that with the increase of fault depth, the strong PGV regions of the FP component gradually depart from the fault trace along the Y direction, and the strong PGVs locate generally in two place. One is the epicentral region, and the other one is the terminal area of the fault right boundary. They are corresponding to the initial and terminal rupture positions, respectively. Since rupture starts and ends at the two positions abruptly, strong seismic waves will be radiated there. Meanwhile, the ground motions of the FP component are most sensitive to the rupture process close to the observation points [8], so the strong PGVs of the FP component will appear at the above two positions. Considering the source radiation pattern of the FP component and the unilateral rupture process, the strong PGV regions near the epicenter show a 45° angle toward the fault trace, and its area is relatively small. However, the strong PGV regions near the right terminal zone of the fault trace have an angle less than 45°, but with a larger area.

Fig. 6 presents the variations of PGV values of the FN component for the stations of line I under different fault depth. It is shown that, with the increase of fault depth, the PGV values from 0 to 40 km decrease rapidly. Beyond this range, the PGVs at the surface become insensitive to the fault depth, and the lines are close to each other for varying source depth. This implies that the fault depth mainly influences the near-field ground motion, and has little effect on the far-field seismic motion. It should be noted that, with the increase of fault depth, the falloff speed after the maximum PGV value gradually becomes slow, and the X coordinate of the maximum PGV moves forward along the positive X axis, which is in accordance with the above analysis that the strong PGVs of the FN component will move forward along the rupture direction with the increasing fault depth.
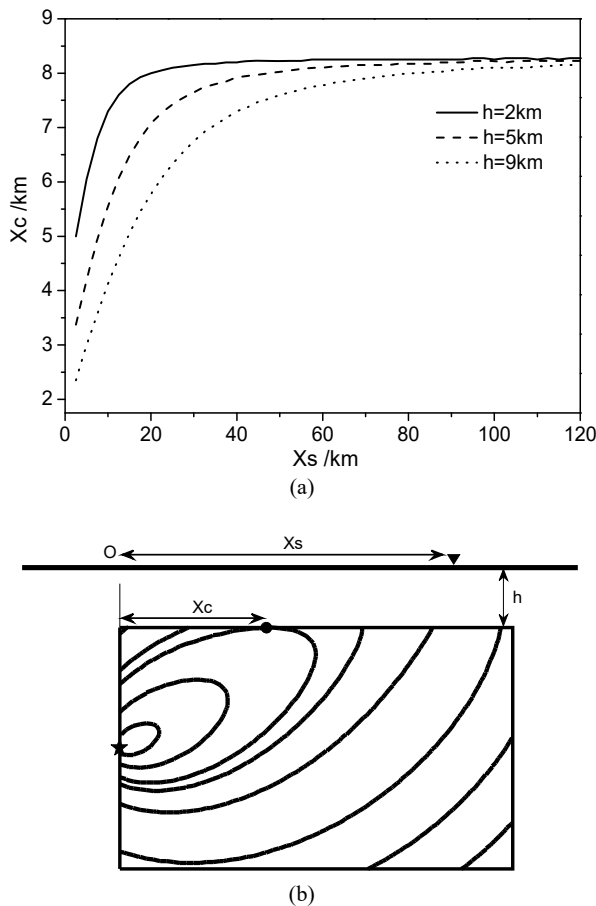
(a)

(b)

Fig. 5 (a) The relation curves between the X coordinates (Xs) of the observation points in line I and their corresponding critical points' X coordinates (Xc) for different fault depth. The value of Xc is approximately unchanged after a point of the curve, and the point is called the limiting position of the critical point. (b) Illustration of Xs and Xc. The mark "▼" indicates the position of observation point, and "●" denotes the critical point. The curves on the fault are isochrone, the point at which the isochrone is tangent to the top of the fault is the critical point
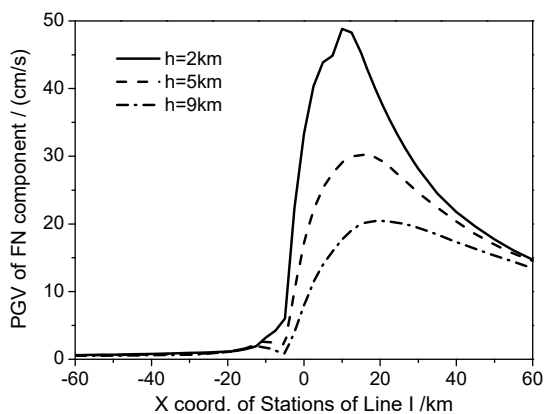

Fig. 6 The variation curve of PGV FN component for observation points of line I with different fault depth

Fig. 7 shows the decrease percentage of maximum PGV value of all stations on the FN and FP component for varying source depth compared with the results of 2 km source depth case. The minus indicates that the PGV value is decreased. It can be found that the fault depth has significant effect on both the FP and FN component PGVs, and the maximum PGV value decreases rapidly with the fault depth. For instance, the maximum PGV value reduces about 60% when the fault depth changes from 2 km to 9 km.
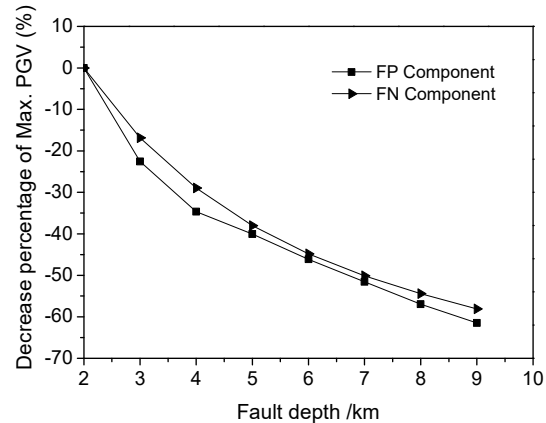

Fig. 7 The decrease rate of PGV maximum for increased fault depth divided by that of h=2 km case

V. CONCLUSIONS

In this study, a vertical strike-slip fault model and a simple homogeneous halfspace model were established first, then the effect of fault depth on near fault PGV was investigated by using the numerical simulation method, and the inherent reason was also discussed. The following basic conclusions can be reached.

1. For the vertical strike-slip fault, the PGV of the FN component is much larger than that of the FP component, which is also validated by the previous studies and the observations.
2. With the increase of fault depth, the maximum value of PGV and the area of strong ground motion reduce rapidly for both the FN and FP component.
3. For the FN component, strong PGVs mainly locate in front of the rupture direction, and the maximum PGV occurs just at the fault trace in front of the rupture direction. With the increase of fault depth, the strong PGV regions move forward along the rupture direction.
4. For the FP component, the strong PGVs locate generally at the epicentral region and the terminal area of the fault right boundary. With the increase of fault depth, the strong PGV regions gradually depart from the fault trace along the FN direction.

The results show that the fault depth has obvious influence on both the FN and FP component of the near field PGV.

REFERENCES

[1] Wang Xiuying, Wang Dengwei. "Relationships between the Wenchuan

earthquake-induced landslide and peak ground velocity, Sichuan, China". *Geological Bulletin of China*, 2011,30(1):159-165.

[2] Wu, Y., Teng, T., Shin, T. and Hsiao, N. "Relationship between peak ground acceleration, peak ground velocity, and intensity in Taiwan", *Bull. Seism. Soc. Am.*, 2003, 93(1): 386–396.

[3] Wald, D. J., Quitoriano, V., Heaton, T. H. and Kanamori, H. 1999a. "Relationships between peak ground accelera- tion, peak ground velocity, and Modified Mercalli Intensity in California". *Earthquake Spectra*, 15(3): 557-564.

[4] Trifunac, M. D. 1995. "Empirical criteria for liquefaction in sands via standard penetration tests and seismic wave energy". *Soil Dynamics & Earthquake Engineering*, 14(6): 419-426.

[5] O'Rourke, M. J. and Ayala, G. "Pipeline damage due to wave propagation". *Journal of Geotechnical Engineering*, 1993, 119(9):1490-1498.

[6] Inoue, T. and T. Miyatake. "3D simulation of near-field strong ground motion based on dynamic modeling". *Bull. Seism. Soc. Am.*, 1998, 88(6): 1445-1456.

[7] Aagaard, B. T., J. F. Hall and T. H. Heaton. "Characterization of near-source ground motions with earthquake simulations". *Earthquake Spectra*, 2001,17(2):177-207.

[8] J. Schmedes and R. J. Archuleta. "Near-source ground motion along strike slip faults: insights into magnitude saturation of PGV and PGA". *Bull. Seism. Soc. Am.*, 2008, 98(5): 2278- 2290.

[9] Olson, A. H., Orcutt, J. A., Frazier, G. A.," The discrete wave number / finite element method for synthetic seismograms". *Geophys. J. R. Astr.Soc.*,1984,77:421-460.

[10] Paul Spudich, R. J. Archuleta. "Techniques for earthquake ground motion calculation with applications to source parameterization of finite faults". in Bolt, B. A. ed., Seismic strong motion synthetics. Orlando, Florida, Academic Press. 205- 265.

[11] Liu Qifang, Yuan Yifan, Jin Xing, et al. "Basic characteristics of near-fault ground motion". *Journal of Earthquake Engineering and Engineering Vibration*, 2006,26(1):1-10.

[12] P. G. Somerville, N. F. Smith, R. W. Graves et al. "Modification of empirical strong ground motion attenuation relations to include the amplitude and duration effects of rupture directivity". *Seism. Res. Lett.*, 1997, 68(1): 199-222.